

Alma Mater Studiorum Università di Bologna  
Archivio istituzionale della ricerca

Millimeter wave free-jet spectrum of the isotopologues of 1,2-butanediol

This is the final peer-reviewed author's accepted manuscript (postprint) of the following publication:

*Published Version:*

Maris A., Favero L.B., Vigorito A., Calabrese C., Evangelisti L., Melandri S. (2020). Millimeter wave free-jet spectrum of the isotopologues of 1,2-butanediol. JOURNAL OF MOLECULAR STRUCTURE, 1205, 127643-127648 [10.1016/j.molstruc.2019.127643].

*Availability:*

This version is available at: <https://hdl.handle.net/11585/781964> since: 2020-12-15

*Published:*

DOI: <http://doi.org/10.1016/j.molstruc.2019.127643>

*Terms of use:*

Some rights reserved. The terms and conditions for the reuse of this version of the manuscript are specified in the publishing policy. For all terms of use and more information see the publisher's website.

This item was downloaded from IRIS Università di Bologna (<https://cris.unibo.it/>).  
When citing, please refer to the published version.

(Article begins on next page)

This is the final peer-reviewed accepted manuscript of:

Maris, A., Favero, L. B., Vigorito, A., Calabrese, C., Evangelisti, L., & Melandri, S. (2020). Millimeter wave free-jet spectrum of the isotopologues of 1, 2-butanediol. *Journal of Molecular Structure*, 1205, 127643.

The final published version is available online at:

<https://doi.org/10.1016/j.molstruc.2019.127643>

© 2020. This manuscript version is made available under the Creative Commons Attribution-NonCommercial-NoDerivs (CC BY-NC-ND) 4.0 International License (<http://creativecommons.org/licenses/by-nc-nd/4.0/>)

# Millimeter wave free-jet spectrum of the isotopologues of 1,2-butanediol

Assimo Maris<sup>a</sup>, Laura B. Favero<sup>b</sup>, Annalisa Vigorito<sup>a</sup>, Camilla Calabrese<sup>c,d</sup>, Luca Evangelisti<sup>a</sup>, Sonia Melandri<sup>a,\*</sup>

<sup>a</sup> Dipartimento di Chimica "G. Ciamician" Dell'Università, Via Selmi 2, I-40126, Bologna, Italy

<sup>b</sup> Istituto per Lo Studio Dei Materiali Nanostrutturati, Sezione di Bologna, Consiglio Nazionale Delle Ricerche (CNR), Via Gobetti 101, I-40129, Bologna, Italy

<sup>c</sup> Departamento Química Física, Facultad de Ciencia y Tecnología Universidad Del País Vasco (UPV/EHU), Apartado 644, E-48080, Bilbao, Spain

<sup>d</sup> Instituto Biofisika (UPV/EHU, CSIC), University of the Basque Country, Leioa, E-48940, Spain

## ARTICLE INFO

### Article history:

Received 6 November 2019

Received in revised form

20 December 2019

Accepted 23 December 2019

Available online 28 December 2019

### Keywords:

1,2-Butanediol

Millimeter wave spectroscopy

Isotopologues

Molecular structure

Interstellar medium

## ABSTRACT

We recorded the rotational spectra of six isotopologues of the most stable conformer of 1,2-butanediol in the 59.6–74.4 GHz frequency region. The observed species are the four monosubstituted <sup>13</sup>C, the OD...OH and the OD...OD, and the measurements were performed using a Free-Jet Absorption Millimeter Wave spectrometer. The analysis of the 18 experimental rotational constants determined for all the isotopologues together with those of the parent species, lead to the determination of the coordinates in the principal axis system for the substituted atoms. From the theoretical structure, calculated at the B3LYP-D3/aug-cc-pVTZ level of theory, a refinement of the structural parameters led to a partial *r*<sub>0</sub> geometry, which reproduced all the rotational constants within 1.3 MHz.

## 1. Introduction

Diols belong to an important class of chemical compounds with several applications and particular characteristics. Regarding their reactivity, diols are used in the synthesis of polyurethanes and polyesters and have recently attracted the attention for these applications in the bio-based industry [1,2], they are also used in cryopreservation [3] and as stabilizers for proteins [4]. Diols are also related and bear similarity to biological building block molecules such as sugar alcohols, therefore there is particular interest in the study of their structures and conformations [5–12], intra- and inter-molecular interactions [6,8–10,12], vibrational motions [13–16] and chirality [15,17]. As complex organic molecules (COMs) and constituents of biological building blocks there is also considerable interest in the search of diols in space because of their implications in the question about the origin of life [18]. Laboratory rotational spectroscopy data in the microwave, millimeter and submillimeter wavelength are necessary for the unique

identification of the molecules in astronomical observations or surveys, and based on their rotational frequencies, more than 200 molecules have been identified in space [19–21]. Rotational spectroscopy performed in supersonic expansions have been proved to be particularly suitable to investigate complex spectra generated by molecules [22] and weakly bound molecular complexes [23,24]. In particular, those experiments allow to identify multiple conformers of a flexible molecule [25], different tautomers [26,27] and different isotopologues [28].

The study of the different isotopologues of a molecule is of importance for different reasons. From a structural point of view, the analysis of the changes in the rotational constants upon isotopic substitution, allows the determination of the position of the substituted atoms without any *a priori* assumptions [29]. If the collection of a complete set of data including all the isotopes is not possible to achieve, a partial structure can be obtained by refining a structure obtained as result of quantum chemical calculations to reproduce all experimental data [30]. From an astrochemical point of view the detected abundance of different isotopologues of a molecular species can give additional information on reaction mechanisms of formation [31] or on the environment in which the molecule is found or formed [32].

\* Corresponding author. Dipartimento di Chimica "G. Ciamician", via Selmi, 2, 40126, Bologna.

E-mail address: [sonia.melandri@unibo.it](mailto:sonia.melandri@unibo.it) (S. Melandri).

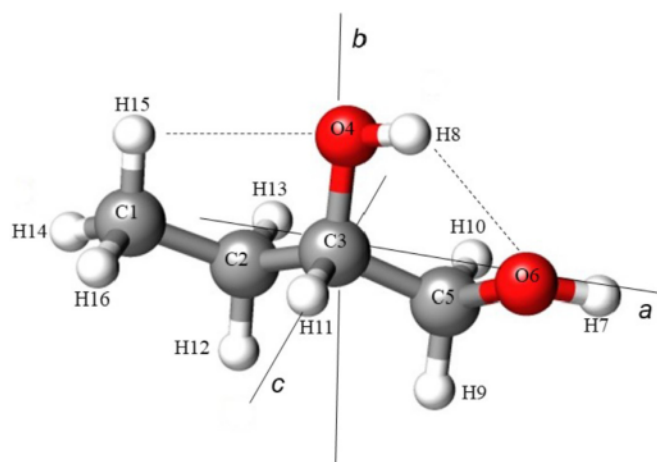


**Fig. 1.** Theoretical (B3LYP-D3/aug-cc-pVTZ) structure of 12BDT drawn by means of the UCSF Chimera program [56].

Diols are particular important in the context of astrochemistry because of their similarity with important biological building block molecules such as sugar alcohols. Ethylene glycol, the simplest diol, being constituted by ten atoms, is one of the largest COMs detected in space so far, as attested by the Cologne Database for Molecular Spectroscopy [19–21].

Higher order diols have all been studied in the laboratory and different propanediols have been searched for in several astronomical surveys but they have not yet been detected (for a complete discussion see Ref. [33] and references therein). Regarding the spectroscopy of diols, rotational spectroscopy investigations are reported for all diols with a linear carbon chain containing up to four carbon atoms. Besides 1,2-butanediol (12BDT) [33], which is the object of this study, the following molecules have been investigated: ethylene glycol or 1,2-ethanediol [5,13,14,34–37], 1,2-propanediol [6,9,38,39], 1,3-propanediol [8,15], 1,3-butanediol [7,10], 2,3-butanediol [17], and 1,4-butanediol [12]. Even though diols may exist in several distinct conformations, the more stable structures are those stabilized by the intramolecular hydrogen bond between the two hydroxyl groups and actually, only this family of conformers was detected in all cited studies by laboratory rotational spectroscopy.

In this paper, we continue our investigation on the most stable conformer of 12BDT and report the analysis of the rotational spectra of all mono-substituted  $^{13}\text{C}$  isotopologues and two deuterium enriched species observed with a Free Jet Absorption Millimeter Wave (FJ-AMMW) spectrometer working in the 59.6–74.4 GHz frequency range.

## 2. Experimental methods

The rotational spectrum of 12BDT ( $\text{C}_4\text{H}_{10}\text{O}_2$ ) was recorded in the 59.6–74.4 GHz region using a Stark-modulated FJ-AMMW spectrometer with a resolution of about 300 kHz and estimated uncertainties for the measurements of about 50 kHz. The main features of the spectrometer have been previously described [33,40,41].

12BDT (purity 98%, molecular weight 90.121 g/mol) was purchased from Sigma-Aldrich and used without any further purification. It appears as a colorless, viscous liquid at ambient conditions. The melting point is  $-50^\circ\text{C}$  (223 K) and the boiling point is  $191\text{--}192^\circ\text{C}$  (464–465 K). Argon, purchased from SIAD (Società Italiana Acetilene e Derivati), was used as carrier gas.

The sample was heated to about  $80^\circ\text{C}$  (353 K) and a stream of Argon ( $P_0 = 20\text{ kPa}$ ) was flowed over it and then expanded to about  $P_b = 0.5\text{ Pa}$  through a heated 0.3 mm diameter pinhole nozzle. In the same conditions,  $\text{D}_2\text{O}$  at a concentration of about 1% was added to the flux of Ar to generate the hydroxyl deuterated species. Relative intensity measurements on the observed Q-branch bands of the parent species match with a rotational temperature of the jet of 3 K in Argon expansion [33].

## 3. Results and discussion

The conformational space of 12BDT was analyzed in detail with quantum chemical methods at the B3LYP-D3/aug-cc-pVTZ level of theory in our previous work [33]. All conformations characterized by the stabilizing hydrogen bond between the hydroxyl groups were optimized and the relative spectroscopic parameters derived theoretically. Based on those calculated data, the spectra of six different conformers were recognized in the 59.6–74.4 GHz range, allowing for the assignment and the determination of the rotational and centrifugal distortion constants. Among the observed species, the signals of the lowest energy one (depicted in Fig. 1, where the atom numbering and the orientation of the principal axes system,

**Table 1**  
Experimental transition frequencies ( $\nu$ ) and residuals ( $\text{o-c}$ ), all in MHz, of 12BDT  $^{13}\text{C}$  isotopologues.

$J'$	$K_a'$	$K_c'$	$J$	$K_a$	$K_c$	$^{13}\text{C}(1)$		$^{13}\text{C}(2)$		$^{13}\text{C}(3)$		$^{13}\text{C}(5)$	
						$\nu$	$\text{o-c}$	$\nu$	$\text{o-c}$	$\nu$	$\text{o-c}$	$\nu$	$\text{o-c}$
5	5	<sup>a</sup>	4	4	*	72176.83	0.03	71678.13	−0.01	72228.63	0.03	71630.28	0.00
5	4	1	4	3	2	60083.71	0.04	59761.99	−0.11	60217.56	−0.07	59727.40	0.00
5	4	2	4	3	1			59760.96	0.05	60216.57	0.13	59726.27	0.08
6	4	2	5	3	3	63633.10	−0.04	63371.30	0.06	63851.38	0.00	63338.77	−0.04
6	4	3	5	3	2	63629.06	−0.01	63366.51	0.07	63846.57	−0.06	63333.88	−0.06
7	4	3	6	3	4	67181.53	0.06	66979.37	0.08	67484.01	−0.03	66949.22	0.10
7	4	4	6	3	3	72228.60	0.0	66964.76	−0.06		0.03	66934.37	−0.10
8	4	4	7	3	5	70729.02	−0.04	70550.47	−0.09	71116.21	−0.08	70559.00	0.01
8	4	5	7	3	4	70698.19	−0.10			71080.18		70522.18	−0.05
9	4	5	8	3	6	74277.30	−0.04	74195.86	0.04			74170.34	0.04
9	4	6	8	3	5	74209.52	0.04	74115.73	−0.06			74089.30	0.04
9	3	6	8	2	7	62811.80	0.06	62978.41	−0.04	63434.12	0.05	62971.81	−0.02
9	3	7	8	2	6	61196.79	0.05	61188.00	0.08	61651.03	0.02	61167.16	−0.01
10	3	7	9	2	8	66718.40	−0.01	66987.51	0.03	67465.63	−0.01	66986.60	0.01
10	3	8	9	2	7	64208.34	−0.01	64209.09	−0.04	64698.41	0.00	64186.69	0.01
9	3	6	8	2	7	62811.80	0.06	62978.41	−0.04	63434.12	0.05	62971.81	−0.02
9	3	7	8	2	6	61196.79	0.05	61188.00	0.08	61651.03	0.02	61167.16	−0.01

<sup>a</sup> Asterisks indicate asymmetry degenerate transition.



PAS, are also indicated) were particularly intense. As a continuation of this previous study, the rotational spectra originating from different isotopologues of this conformer, were searched for in the recorded spectrum. The overall intensity of the spectrum allowed indeed the observation of the transitions originating from the four  $^{13}\text{C}$  mono-substituted isotopologues (see Fig. 1) in natural abundance while the deuterated enriched species were generated with the procedure described in the previous section. For the parent species, the transitions observed in the spectrometer's frequency range were  $\mu_a$  R-type transitions with rotational quantum number  $J$  ranging from 9 to 13 and  $K_a$  from 0 to 10,  $\mu_b$  R-type transitions with rotational quantum number  $J$  ranging from 5 to 28 and  $K_a$  ranging from 0 to 8 and  $\mu_c$  R-type transitions with rotational quantum number  $J$  ranging from 5 to 20 and  $K_a$  from 1 to 8. The natural abundance of  $^{13}\text{C}$  is about 1%, thus only the most intense lines were observed in the spectrum for the mono-substituted species while many more lines were observed for the deuterium enriched samples. The transitions were fitted via Pickett's SPFIT program [42] using a standard Hamiltonian containing quartic centrifugal distortion constants and, because 12BTD is a near-prolate asymmetric top, the  $S$ -reduction and  $J'$ -representation were selected [43]. All the measured transitions are reported in Tables 1 and 2 while the fitted spectroscopic parameters for the parent species and all the observed isotopologues can be found in Table 3. The fact that only one deuterated species (the one with the deuterium involved in the hydrogen bond) could be observed, is puzzling but similar phenomena have been observed in weakly bound hydrogen bonded cluster where in several cases it was impossible to observe the species deuterated on the free hydrogen. This is generally attributed to the higher stability of the deuterium bond over the hydrogen bond [44,45].

The determined rotational constants together with those of the parent species [33], allowed the calculation of the  $r_s$  structure through Kraitchman's substitution method [46]. This analysis determined the coordinates of the substituted atoms in the PAS of the reference species from the changes in the principal moments of inertia, resulting from a single isotopic substitution. The main assumption of this analysis is that the observed structures are not affected by the mass dependence of the vibrations of the molecule and that the inertial axes are not significantly shifted by the change in mass. The  $r_s$  coordinates for all monosubstituted atoms are reported in the first column of Table 4. Regarding the doubly hydroxyl deuterated species, the reference molecule was assumed to be the mono-deuterated one. The  $r_s$  coordinates for these two hydrogens in the corresponding PAS are reported in Table 5. The inspection of the results reported in Tables 4 and 5 show that the substitution method fails to reproduce the position of the atoms when the coordinate is very close to zero. In these cases the square of the coordinate which is determined from the method is small and negative and gives an imaginary value of the coordinate itself.

Another approach to structure determination, consists in performing a refinement of the structural parameters to reproduce the observed rotational constants of all the isotopologues ( $r_0$ ). As a starting point for the least-squares structural refinement, we used the theoretically calculated internal coordinates for the molecule at the B3LYP-D3/aug-cc-pVTZ level ( $r_e$ ) and refined the most significant structural parameters using Kisiel's STRFIT program [47]. 14 structural parameters were adjusted: the 3 C–C bond distances, 6 valence angles and 5 dihedral angles. As a result of the fitting procedure, the rotational constants for the four  $^{13}\text{C}$  and the monodeuterated species were reproduced within 0.8 MHz, while those of the double deuterated species within 1.3 MHz. The theoretical ( $r_e$ ) and fitted structural parameters ( $r_0$ ) are reported in Table 6.

Moreover, in Table 4, we compare  $r_s$  (absolute values), the  $r_0$  and the  $r_e$  coordinates of the substituted atoms. Although a direct

**Table 2**

Experimental transition frequencies ( $\nu$ ) and residuals (o-c), all in MHz, of 12BTD deuterated isotopologues.

$J'$	$K_a'$	$K_c'$	$J$	$K_a$	$K_c$	D(8)		D(7) & D(8)	
						$\nu$	o-c	$\nu$	o-c
7	7	*	7	6	*	74151.52	0.05		
8	7	*	8	6	*	74144.68	0.03		
9	7	*	9	6	*	74135.03	−0.02		
10	7	*	10	6	*	74121.96	−0.03		
11	7	*	11	6	*	74104.65	−0.08		
12	7	*	12	6	*	74082.34	−0.06		
13	7	*	13	6	*	74054.11	0.01		
14	7	*	14	6	*	74018.73	−0.08		
6	6	*	6	5	*	62745.00	0.08	63216.36	0.04
7	6	*	7	5	*	62737.41	0.07	63209.72	0.03
8	6	*	8	5	*	62726.17	0.04	63199.92	0.03
9	6	*	9	5	*	62710.27	0.01	63186.03	−0.01
10	6	*	10	5	*	62688.58	0.02	63167.08	−0.04
11	6	*	11	5	*	62659.84	0.11	63141.94	−0.06
12	6	7	12	5	8	62622.92	−0.03		
12	6	6	12	5	8	62622.92	−0.05		
5	5	*	4	4	*	69402.04	0.11	69182.85	−0.05
6	5	*	5	4	*	73013.04	−0.01	72673.37	0.10
6	4	3	5	3	2	61597.47	0.09		
6	4	2	5	3	2	61597.47	−0.09		
7	4	4	6	3	3	65194.36	−0.03	64651.56	−0.08
7	4	3	6	3	3	65195.14	0.09	64652.24	0.10
7	4	4	6	3	4	65212.43	−0.09	64666.23	−0.07
7	4	3	6	3	4	65213.20	0.02	64666.89	0.09
8	4	5	7	3	4	68775.76	−0.05	68117.01	−0.09
8	4	4	7	3	4	68777.77	−0.02	68118.61	0.02
8	4	5	7	3	5	68820.96	0.00	68153.57	−0.06
8	4	4	7	3	5	68823.02	0.08	68155.18	0.06
9	4	6	8	3	5	72331.72	−0.04	71561.35	0.02
9	4	5	8	3	6	72435.55	−0.10	71565.23	0.05
9	4	6	8	3	6			71641.25	−0.04
9	4	5	8	3	6			71645.11	−0.03
9	3	7	8	2	6	59757.80	−0.04		
9	3	6	8	2	6	59953.68	−0.02		
9	3	7	8	2	7	61653.81	−0.01	60704.70	−0.02
9	3	6	8	2	7	61849.63	−0.05	60863.45	−0.04
10	3	8	9	2	7	62699.67	−0.05	61936.00	0.01
10	3	7	9	2	7			62227.89	0.01
10	3	8	9	2	8			64470.21	−0.03
10	3	7	9	2	8	65935.72	0.01	64762.10	−0.03
11	3	9	10	2	8	65458.47	0.01	64661.95	−0.03
11	3	8	10	2	9	70209.98	−0.02	68822.32	0.04
12	3	10	11	2	9	68033.95	0.04	67215.48	−0.03
12	3	9	11	2	10			73084.18	0.01
13	3	11	12	2	10	70434.35	−0.07	69601.43	0.04
14	3	12	13	2	11			71830.73	0.00
15	3	13	14	2	12			73919.19	0.05
10	2	8	9	1	9	63426.14	0.00	61491.28	0.00
11	2	9	10	1	10	69920.03	0.01		
15	2	13	14	1	13			71143.91	0.03
16	2	15	15	1	14			60230.33	0.01
17	2	16	16	1	15			62619.96	−0.01
18	2	17	17	1	16			65101.51	−0.03
17	1	16	16	1	15	60955.14	0.05		
17	2	16	16	2	15	60172.96	−0.01	61111.83	0.01
17	2	15	16	2	14	63217.43	0.03		
17	3	15	16	3	14	61483.49	0.09		
17	3	14	16	3	13	63092.07	0.04	60833.74	0.04
17	4	14	16	4	13	61789.51	−0.01	59696.44	−0.02
17	4	13	16	4	12	62063.05	−0.02	59905.76	−0.04
17	5	13	16	5	12	61698.36	−0.09		
17	5	12	16	5	11	61717.20	−0.03		
18	0	18	17	0	17	61353.09	0.05		
18	1	18	17	1	17	61306.13	0.03		

<sup>a</sup> Asterisks indicate asymmetry degenerate transitions.

comparison between theoretical structures (referring to the  $r_e$  equilibrium geometry) and experimental data ( $r_0$ , related to the ground vibrational state) must be considered with care, it is worth noting that many of the structural parameters are quite consistent.

**Table 3**  
Spectroscopic constants for six isotopic species of 12BTD.

	$^{13}\text{C}(1)$	$^{13}\text{C}(2)$	$^{13}\text{C}(3)$	$^{13}\text{C}(5)$	D(8)	D(7) & D(8)
A/MHz	7822.819(4) <sup>a</sup>	7764.091(3)	7823.890(3)	7758.649(3)	7493.450(4)	7511.096(2)
B/MHz	1896.985(3)	1932.312(3)	1944.863(3)	1933.875(3)	1871.4086(6)	1940.3000(5)
C/MHz	1651.512(3)	1675.606(3)	1687.690(3)	1676.288(3)	1616.9506(6)	1668.4585(5)
$D_K/\text{kHz}^b$					7.45(8)	7.96(4)
$N^c$	14	14	12	15	42	51
$r_{\text{rms}}^d/\text{kHz}$	47	61	55	50	46	52

<sup>a</sup> Errors in parentheses are expressed in units of the last digit.  
<sup>b</sup> Quartic centrifugal distortion constants fixed to the values of the parent species ( $D_J = 0.16080(41)$ ,  $D_{JK} = 1.9773(25)$ ,  $D_K = 8.253(16)$ ,  $d_1 = -0.01813(15)$ ,  $d_2 = -0.00406(13)$  kHz) [33], unless otherwise specified.  
<sup>c</sup> Number of distinct frequency lines in the fit.  
<sup>d</sup> Root mean square deviation of the fit.

**Table 4**  
Comparison between  $r_s$ ,  $r_0$ ,  $r_e$  coordinates (Å) for substituted atoms for 12BTD.

		$r_s^a$	$r_0$	$r_e$
C1	a	2.5665(6) <sup>b</sup>	−2.569(1)	−2.571
	b	0.03(6)	−0.029(4)	−0.035
	c	0.248(6)	0.254(4)	0.257
C2	a	1.291(1)	−1.297(2)	−1.298
	b	0.698(2)	−0.670(5)	−0.700
	c	0.265(6)	−0.261(4)	−0.263
C3	a	i0.129 <sup>c</sup>	−0.033(5)	−0.031
	b	i0.067	−0.016(3)	−0.015
	c	0.237(6)	0.227(9)	0.228
C5	a	1.215(1)	1.222(2)	1.224
	b	0.745(2)	−0.748(4)	−0.739
	c	0.220(7)	−0.218(7)	−0.231
H8	a	0.815(2)	0.820(6)	0.826
	b	1.6689(9)	1.665(3)	1.707
	c	i0.145	0.04(2)	−0.053

<sup>a</sup>  $r_s$  coordinates are absolute values.  
<sup>b</sup> Errors in parentheses are expressed in units of the last digit. For  $r_s$  Constrain's errors [57] are given.  
<sup>c</sup> In a few cases the square of the coordinate has been determined to be small and negative leading to an imaginary value of the coordinate.

**Table 5**  
 $r_s$  coordinates (Å, absolute values) for substituted hydrogen atoms for 12BTD in the PAS of the D8-12BTD.

	H7	H8
a	3.0947(5)	0.817(2)
b	0.340(4)	1.6440(9)
c	0.226(7)	i0.133

**Table 6**  
 $r_e$  structure (B3LYP-D3/aug-cc-pVTZ) of 12BTD compared to effective  $r_0$  structure.

Bond distances/Å			Valence angles/°			Dihedral angles/°		
	$r_0^a$	$r_e$		$r_0$	$r_e$		$r_0$	$r_e$
C1C2	1.528(3) <sup>b</sup>	1.5274						
C2C3	1.517(4)	1.5216	C1C2C3	112.8(5)	112.89			
C3O4		1.4266	C2C3O4	108.4(1)	108.08	C1C2–C3O4	62.0(8)	61.83
C5C3	1.519(3)	1.5197	C2C3C5	112.1(5)	112.10	C1C2–C3C5	−176.2(5)	−176.58
C5O6		1.4326	C3C5O6	106.95(5)	107.13	C2C3–C5O6	−178.9(9)	−179.79
O6H7	0.9602	0.9602	C5O6H7	106.1(4)	109.65	C3C5–O6H7	164(1)	166.28
O4H8	0.9638	0.9638	C3O4H8	103.1(4)	107.27	C5C3–O4H8	54(1)	49.39
C5H9	1.0953	1.0953	C3C5H9		109.95	O4C3–C5H9		−179.77
C5H10	1.0949	1.0949	C3C5H10		109.18	O4C3–C5H10		60.58
C3H11	1.0994	1.0994	C5C3H11		107.77	O6C5–C3H11		59.89
C2H12	1.0933	1.0933	C3C2H12		108.49	C5C3–C2H12		−54.40
C2H13	1.0933	1.0933	C3C2H13		108.26	C5C3–C2H13		61.54
C1H14	1.0905	1.0905	C2C1H14		111.02	C3C2–C1H14		−179.63
C1H15	1.0888	1.0888	C2C1H15		110.65	C3C2–C1H15		−59.29
C1H16	1.0919	1.0919	C2C1H16		110.94	C3C2–C1H16		60.43

<sup>a</sup> Only the fitted parameters are reported. In the fitting procedure, all the other parameters were kept fixed to the theoretical ones.  
<sup>b</sup> Errors in parentheses are expressed in units of the last digit.

A few adjustments had to be made to the theoretical B3LYP-D3/aug-cc-pVTZ structure to reproduce the experimental rotational constants. The structural parameters that are mainly affected are the valence and dihedral angles, namely C5O6H7, C3O4H8 and C5C3O4H8, of the atoms involved in the hydrogen bond, which show deviations up to 5°.

The geometry of the most stable conformer of 12BTD is stabilized by a 5-atom ring like structure held together by an intramolecular hydrogen bond (H···O) with a relatively short length: the  $r_0$  and  $r_e$  values are 2.27(2) Å and 2.31 Å respectively which is shorter than the sum of their van der Waals radii (2.70 Å) [48]. Similar ring structures have been observed to be typical of small linear diols isolated in the gas phase: 5-membered rings are formed in smaller vicinal diols such as ethylene glycol [5] and 1,2-propanediol [6,9], 6-membered rings in 1,3-propanediol [7,8] and 1,3-butanediol [10] and 7-membered ones in 1,4-butanediol [12]. The patterns are maintained when a hydrogen bond donor and acceptor are present in the same molecules such as in 1,2-aminoethanol [49] or N-methyl-2-aminoethanol [50,51] and also in aromatic systems such as catechol [52,53]. A close inspection of the structure provides evidence of a proximity between the H15 aliphatic hydrogen and the O4 atom: the distance between them is 2.61(3) Å (both  $r_0$  and  $r_e$  values). This short distance could be the signature of a weak hydrogen bond [54], which is responsible for the stabilization of the conformer.

From the  $r_s$  coordinates of the hydroxyl hydrogen atoms given in Table 5, the distance between them can be calculated directly provided the imaginary coordinate is set to zero. The obtained value can be compared to that of the other vicinal diols. In 12BTD



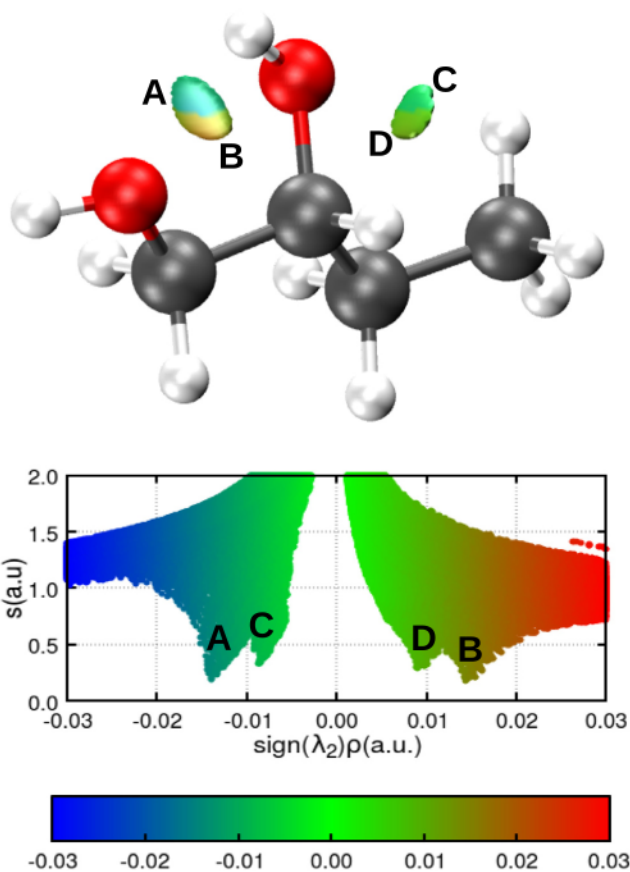


**Fig. 2.** The NCI plots for the studied molecule. Blue and green colors identify the presence of strong and weak attractive interactions, respectively. Red color indicates repulsive interaction.

this distance is 3.029 Å in agreement with the values in 2,3-butanediol (3.032 Å in the heterochiral species and 3.014 Å in the homochiral one) [17], 1,2-propanediol (3.076 Å) [9] and that in ethylene glycol (3.009 Å) [5] or in catechol (3.037 Å) [52].

A visualization of the non-covalent interactions was achieved with the NCI method [55], which considers the distribution of both the electron density ( $\rho$ ), and its gradient ( $\sigma$ ) and its second derivatives matrix ( $\lambda_1, \lambda_2, \lambda_3$ ). A comprehensive picture can be drawn using different plots of these quantities (see Fig. 2). According to the color code reported on the graphics, the isosurfaces visible in the NCI plots represent the area for attractive and repulsive interactions. From the picture it can be seen that indeed an attractive O—H...O and a weaker C—H...O are present.

#### 4. Conclusions

We report the millimeter wave transition frequencies for four mono-substituted  $^{13}\text{C}$  isotopologues and two deuterated species of the lowest energy conformer of 12BTD. This study can be considered an additional step in the extensive study of diols, which could lead to their astronomical detection and the measurement of their isotopic abundances in the interstellar medium. This search has been extensive after the detection of the related molecule ethylene glycol (see Ref. [33] and references therein).

Moreover, the analysis of the experimental rotational constants determined for all the isotopologues led to the determination of the substitution coordinates for these atoms. Also, from the theoretical

calculated structure a refinement of the structural parameters led to a partial  $r_0$  geometry which reproduced all the rotational constants within less than 1.3 MHz.

#### CRediT authorship contribution statement

**Assimo Maris:** Conceptualization, Investigation, Writing - original draft, Writing - review & editing. **Laura B. Favero:** Formal analysis, Writing - review & editing. **Annalisa Vigorito:** Investigation, Data curation, Writing - review & editing. **Camilla Calabrese:** Investigation, Data curation, Writing - review & editing. **Luca Evangelisti:** Conceptualization, Writing - original draft, Writing - review & editing. **Sonia Melandri:** Conceptualization, Writing - original draft, Writing - review & editing.

#### Acknowledgments

The authors thank the University of Bologna for financial support (RFO), and the CINECA award under the ISCRA initiative, for the availability of high-performance computing resources and support. C.C. acknowledges the Spanish Government for a “Juan de la Cierva” contract.

#### References

- [1] K. Tachibana, H. Abe, Studies on thermo-mechanical and thermal degradation properties of bio-based polyurethanes synthesized from vanillin-derived diol and lysine diisocyanate, *Polym. Degrad. Stab.* 167 (2019) 283–291, <https://doi.org/10.1016/j.polymdegradstab.2019.07.014>.
- [2] M. Gomes, A. Gandini, A.J.D. Silvestre, B. Reis, Synthesis and characterization of poly(2,5-furan dicarboxylate)s based on a variety of diols, *J. Polym. Sci. A Polym. Chem.* 49 (2011) 3759–3768, <https://doi.org/10.1002/pola.24812>.
- [3] H.T. Meryman, Cryopreservation of living cells: principles and practice, *Transfusion* 47 (2007) 935–945, <https://doi.org/10.1111/j.1537-2995.2007.01212.x>.
- [4] N. Kishore, R. Marathe, Volumetric properties and surface tension of aqueous 3-chloropropan-1-ol and aqueous 3-chloropropan-1,2-diol, and correlation of their effect on protein stability, *J. Chem. Thermodyn.* 32 (2000) 413–424, <https://doi.org/10.1006/jcht.2000.0624>.
- [5] W. Caminati, G. Corbelli, Conformation of ethylene glycol from the rotational spectra of the nontunneling O-monodeuterated species, *J. Mol. Spectrosc.* 90 (1981) 572–578, [https://doi.org/10.1016/0022-2852\(81\)90146-6](https://doi.org/10.1016/0022-2852(81)90146-6).
- [6] W. Caminati, Conformation and hydrogen bond in 1,2-propanediol, *J. Mol. Spectrosc.* 86 (1981) 193, [https://doi.org/10.1016/0022-2852\(81\)90117-X](https://doi.org/10.1016/0022-2852(81)90117-X).
- [7] W. Caminati, G. Corbelli, The six-membered ring chair conformation of butane-1,3-diol in the gas phase, *J. Mol. Struct.* 78 (1982) 197, [https://doi.org/10.1016/0022-2860\(82\)80006-9](https://doi.org/10.1016/0022-2860(82)80006-9).
- [8] W. Caminati, S. Melandri, P.G. Favero, Free-jet absorption microwave spectrum of 1,3-propanediol, *J. Mol. Spectrosc.* 171 (1995) 394–401, <https://doi.org/10.1006/jmsp.1995.1128>.
- [9] J.L. Lockley, J.P.I. Hearn, A.K. King, B.J. Howard, Detection and analysis of a new conformational isomer of propan-1,2-diol by Fourier transform microwave spectroscopy, *J. Mol. Struct.* 612 (2002) 199, [https://doi.org/10.1016/S0022-2860\(02\)00090-X](https://doi.org/10.1016/S0022-2860(02)00090-X).
- [10] B. Velino, L.B. Favero, A. Maris, W. Caminati, Conformational equilibria in diols: the rotational spectrum of chiral 1, 3-butanediol, *J. Phys. Chem. A* 115 (2011) 9585, <https://doi.org/10.1021/jp200187f>.
- [11] I.A. Smirnov, E.A. Alekseev, V.I. Pidychiy, V. V. Ilyushin, R.A. Motiyenko, 1,3-Propanediol millimeter wave spectrum: conformers I and II, *J. Mol. Spectrosc.* 293–294 (2013) 33–37, <https://doi.org/10.1016/j.jms.2013.10.001>.
- [12] L. Evangelisti, Q. Gou, L. Spada, G. Feng, W. Caminati, Conformational analysis of 1, 4-butanediol: a microwave spectroscopy study, *Chem. Phys. Lett.* 556 (2013) 55, <https://doi.org/10.1016/j.cplett.2012.11.080>.
- [13] D. Christen, L.H. Coudert, R.D. Suenram, F.J. Lovas, The rotational/concerted torsional spectrum of the g'Ga conformer of ethylene glycol, *J. Mol. Spectrosc.* 172 (1995) 57–77, <https://doi.org/10.1006/jmsp.1995.1155>.
- [14] D. Christen, L.H. Coudert, J.A. Larsson, D. Cremer, The rotational-torsional spectrum of the g'Gg conformer of ethylene glycol: elucidation of an unusual tunneling path, *J. Mol. Spectrosc.* 205 (2001) 185, <https://doi.org/10.1006/jmsp.2000.8263>.
- [15] D.F. Plusquellic, F.J. Lovas, B.H. Pate, J.L. Neill, M.T. Muckle, A.J. Remijan, Distinguishing tunneling pathways for two chiral conformer pairs of 1,3-propanediol from the microwave spectrum, *J. Phys. Chem. A* 113 (2009) 12911–12918, <https://doi.org/10.1021/jp907564y>.
- [16] B.E. Arenas, S. Gruet, A.L. Steber, M. Schnell, A global study of the conformers of 1,2-propanediol and new vibrationally excited states, *J. Mol. Spectrosc.* 337 (2017) 9–16, <https://doi.org/10.1016/j.jms.2017.02.017>.

- [17] J. Paul, I. Hearn, B.J. Howard, Chiral recognition in a single molecule: a study of homo and heterochiral butan-2,3-diol by Fourier transform microwave spectroscopy, *Mol. Phys.* 105 (2007) 825–839, <https://doi.org/10.1080/00268970701241649>.
- [18] E. Herbst, E.F. van Dishoeck, Complex organic interstellar molecules, *Annu. Rev. Astron. Astrophys.* 47 (2009) 427–480, <https://doi.org/10.1146/annurev-astro-082708-101654>.
- [19] CDMS 2001, The Cologne Database for Molecular Spectroscopy, (n.d.). <https://www.astro.uni-koeln.de/cdms/molecules>.
- [20] H.S.P. Müller, S. Thorwirth, D.A. Roth, G. Winnewisser, The Cologne Database for molecular spectroscopy, *CDMS, Astron. Astrophys.* 370 (2001) L49–L52, <https://doi.org/10.1051/0004-6361/20010367>.
- [21] H.S.P. Müller, F. Schlöder, J. Stutzki, G. Winnewisser, The Cologne Database for Molecular Spectroscopy, CDMS: a useful tool for astronomers and spectroscopists, *J. Mol. Struct.* 742 (2005) 215–227, <https://doi.org/10.1016/j.molstruc.2005.01.027>.
- [22] C. Calabrese, Q. Gou, A. Maris, S. Melandri, W. Caminati, Conformational equilibrium and internal dynamics of E-anethole: a rotational study, *J. Phys. Chem. B* 120 (2016), <https://doi.org/10.1021/acs.jpcc.6b04883>.
- [23] L.B. Favero, B.M. Giuliano, A. Maris, S. Melandri, P. Ottaviani, B. Velino, W. Caminati, Features of the C–H...N weak hydrogen bond and internal dynamics in pyridine-CHF<sub>3</sub>, *Chemistry* 16 (2010) 1761–1764, <https://doi.org/10.1002/chem.200902852>.
- [24] B. Velino, S. Melandri, W. Caminati, Internal motions of the rare gas atom in dimethyl Ether–Krypton, *J. Phys. Chem. A* 108 (2004) 4224–4227, <https://doi.org/10.1021/jp0499068>.
- [25] A. Vigorito, C. Calabrese, E. Paltanin, S. Melandri, A. Maris, Regarding the torsional flexibility of the dihydrolipoic acid's pharmacophore: 1,3-Propanedithiol, *Phys. Chem. Chem. Phys.* 19 (2017) 496–502, <https://doi.org/10.1039/c6cp05606g>.
- [26] R. Sanchez, B.M. Giuliano, S. Melandri, L.B. Favero, W. Caminati, Gas-phase tautomeric equilibrium of 4-hydroxypyrimidine with its ketonic forms: a free jet millimeterwave spectroscopy study, *J. Am. Chem. Soc.* 129 (2007) 6287–6290, <https://doi.org/10.1021/ja070712q>.
- [27] S. Melandri, L. Evangelisti, A. Maris, W. Caminati, B.M. Giuliano, V. Feyer, K.C. Prince, M. Coreno, Rotational and core level spectroscopies as complementary techniques in tautomeric/conformational studies: the case of 2-mercaptopyridine, *J. Am. Chem. Soc.* 132 (2010) 10269–10271, <https://doi.org/10.1021/ja104484b>.
- [28] C. Calabrese, A. Vigorito, G. Feng, L.B. Favero, A. Maris, S. Melandri, W.D. Geppert, W. Caminati, Laboratory rotational spectrum of acrylic acid and its isotopologues in the 6–18.5GHz and 52–74.4GHz frequency ranges, *J. Mol. Spectrosc.* 295 (2014) 37–43, <https://doi.org/10.1016/j.jms.2013.11.003>.
- [29] L. Evangelisti, C. Perez, N.A. Seifert, B.H. Pate, M. Dehghany, N. Moazzen-Ahmadi, A.R.W. McKellar, Theory vs. experiment for molecular clusters: spectra of OCS trimers and tetramers, *J. Chem. Phys.* 142 (2015) 104309, <https://doi.org/10.1063/1.4914323>.
- [30] I. Uriarte, S. Melandri, A. Maris, C. Calabrese, E.J. Cocinero, Shapes, dynamics, and stability of  $\beta$ -ionone and its two mutants evidenced by high-resolution spectroscopy in the gas phase, *J. Phys. Chem. Lett.* 9 (2018) 1497–1502, <https://doi.org/10.1021/acs.jpclett.8b00256>.
- [31] J.L. Neill, A.L. Steber, M.T. Muckle, D.P. Zaleski, V. Lattanzi, S. Spezzano, M.C. McCarthy, A.J. Remijan, D.N. Friedel, S.L. Widicus Weaver, B.H. Pate, Spatial distributions and interstellar reaction processes, *J. Phys. Chem. A* 115 (2011) 6472–6480, <https://doi.org/10.1021/jp200539b>.
- [32] M. Imai, N. Sakai, A. López-Sepulcre, A.E. Higuchi, Y. Zhang, Y. Oya, Y. Watanabe, T. Sakai, C. Ceccarelli, B. Lefloch, S. Yamamoto, Deuterium fractionation survey toward protostellar sources in the perseus molecular cloud: HNC case, *Astrophys. J.* 869 (2018) 51, <https://doi.org/10.3847/1538-4357/aab21>.
- [33] A. Vigorito, C. Calabrese, S. Melandri, A. Caracciolo, S. Mariotti, A. Giannetti, M. Massardi, A. Maris, Millimeter-wave spectroscopy and modeling of 1,2-butanediol: laboratory spectrum in the 59.6–103.6 GHz region and comparison with the ALMA archived observations, *Astron. Astrophys.* 619 (2018) A140, <https://doi.org/10.1051/0004-6361/201833489>.
- [34] K.-M. Marstokk, H. Møllendal, On the microwave spectrum of ethylene glycol, *J. Mol. Struct.* 22 (1974) 301, [https://doi.org/10.1016/0022-2860\(74\)85156-2](https://doi.org/10.1016/0022-2860(74)85156-2).
- [35] E. Walder, A. Bauder, H.H. Günthard, Microwave spectrum and internal rotations of ethylene glycol, I. Glycol-O-d<sub>2</sub>, *Chem. Phys.* 51 (1980) 223, [https://doi.org/10.1016/0301-0104\(80\)80098-X](https://doi.org/10.1016/0301-0104(80)80098-X).
- [36] D. Christen, H.S.P. Müller, The millimeter wave spectrum of aGg' ethylene glycol: the quest for higher precision, *Phys. Chem. Chem. Phys.* 5 (2003) 3600, <https://doi.org/10.1039/B304566H>.
- [37] H.S.P. Müller, D. Christen, Millimeter and submillimeter wave spectroscopic investigations into the rotation-tunneling spectrum of gGg' ethylene glycol, HOCH<sub>2</sub>CH<sub>2</sub>OH, *J. Mol. Spectr.* 228 (2004) 298, <https://doi.org/10.1016/j.jms.2004.04.009>.
- [38] F.J. Lovas, D.F. Plusquellic, B.H. Pate, J.L. Neill, M.T. Muckle, A.J. Remijan, Microwave spectrum of 1,2-propanediol, *J. Mol. Spectrosc.* 257 (2009) 82–93, <https://doi.org/10.1016/j.jms.2009.06.013>.
- [39] J.B. Bossa, M.H. Ordu, H.S.P. Müller, F. Lewen, S. Schlemmer, Laboratory spectroscopy of 1, 2-propanediol at millimeter and submillimeter wavelengths, *A&A*, vol. 570, 2014, p. A12, <https://doi.org/10.1051/0004-6361/201424320>.
- [40] C. Calabrese, A. Maris, L. Evangelisti, L.B. Favero, S. Melandri, W. Caminati, Keto-enol tautomerism and conformational landscape of 1,3-cyclohexanedione from its free jet millimeter-wave absorption spectrum, *J. Phys. Chem. A* 117 (2013) 13712–13718, <https://doi.org/10.1021/jp4078097>.
- [41] C. Calabrese, A. Vigorito, A. Maris, S. Mariotti, P. Fathi, W.D. Geppert, S. Melandri, Millimeter wave spectrum of the weakly bound complex CH<sub>2</sub>=CHCN·H<sub>2</sub>O: structure, dynamics, and implications for astronomical search, *J. Phys. Chem. A* 119 (2015) 11674–11682, <https://doi.org/10.1021/acs.jpca.5b08426>.
- [42] H.M. Pickett, Fitting and prediction of vibration-rotation spectra with spin interactions, *J. Mol. Spectrosc.* 148 (1991) 371.
- [43] J.K.G. Watson, in: *Vibrational Spectra and Structure*, vol. vol. I, Elsevier Science Publishers B.V., Oxford, New York, 1977.
- [44] S. Melandri, P.G. Favero, W. Caminati, Detection of the syn conformer of allyl alcohol by free jet microwave spectroscopy, *Chem. Phys. Lett.* 223 (1994) 541–545, [https://doi.org/10.1016/0009-2614\(94\)00478-1](https://doi.org/10.1016/0009-2614(94)00478-1).
- [45] W. Caminati, S. Melandri, I. Rossi, P.G. Favero, The C–F...H–O hydrogen bond in the gas phase. Rotational spectrum and ab initio calculations of difluoromethane-water, *J. Am. Chem. Soc.* 121 (1999) 10098–10101, <https://doi.org/10.1021/ja9907820>.
- [46] J. Kraitchman, Determination of molecular structure from microwave spectroscopic data, *Am. J. Phys.* 21 (1953) 17, <https://doi.org/10.1119/1.1933338>.
- [47] Z. Kisiel, in: J. Demaison, E. Al (Eds.), *Spectroscopy from Space*, Kluwer Academic, Dordrecht, 2001, pp. 91–106.
- [48] S. Alvarez, A cartography of the van der Waals territories, *Dalton Trans.* 42 (2013) 8617–8636, <https://doi.org/10.1039/c3dt50599e>.
- [49] R.E. Penn, R.F. Curl Jr., Microwave spectrum of 2-aminoethanol: structural effects of the hydrogen bond, *J. Chem. Phys.* 55 (1971) 651–658, <https://doi.org/10.1063/1.1676133>.
- [50] L.B. Favero, S. Melandri, P.G. Favero, Microwave spectrum of 35ClCN in excited vibrational states, *Chem. Phys.* 176 (1993) 165–170, [https://doi.org/10.1016/0301-0104\(93\)85014-Y](https://doi.org/10.1016/0301-0104(93)85014-Y).
- [51] S. Melandri, A. Maris, C. Calabrese, L. Evangelisti, A. Piras, V. Parravicini, Rotational spectrum and conformational analysis of N-methyl-2-aminoethanol: insights into the shape of adrenergic neurotransmitters, *Front. Chem.* 6 (2018), <https://doi.org/10.3389/fchem.2018.00025>.
- [52] M. Onda, K. Hasunuma, T. Hashimoto, I. Yamaguchi, Microwave spectrum of catechol (1,2-dihydroxybenzene), *J. Mol. Struct.* 159 (1987) 243–248, [https://doi.org/10.1016/0022-2860\(87\)80042-X](https://doi.org/10.1016/0022-2860(87)80042-X).
- [53] W. Caminati, S. Di Bernardo, L. Schäfer, S.Q. Kulp-Newton, K. Siam, Investigation of the molecular structure of catechol by combined microwave spectroscopy and AB initio calculations, *J. Mol. Struct.* 240 (1990) 263–274, [https://doi.org/10.1016/0022-2860\(90\)80515-L](https://doi.org/10.1016/0022-2860(90)80515-L).
- [54] S. Melandri, "Union is strength": how weak hydrogen bonds become stronger, *Phys. Chem. Chem. Phys.: Phys. Chem. Chem. Phys.* 13 (2011), <https://doi.org/10.1039/c1cp20824a>, 13901–11.
- [55] E.R. Johnson, S. Keinan, P. Mori-Sánchez, J. Contreras-García, W. Cohen, Yang, Revealing noncovalent interactions, *J. Am. Chem. Soc.* 132 (2010) 6498–6506, <https://doi.org/10.1021/ja100936w>.
- [56] E.F. Pettersen, T.D. Goddard, C.C. Huang, G.S. Couch, D.M. Greenblatt, E.C. Meng, T.E. Ferrin, UCSF Chimera—a visualization system for exploratory research and analysis, *J. Comput. Chem.* 25 (13) (2004) 1605–1612, <https://doi.org/10.1002/jcc.20084>.
- [57] C.C. Costain, Determination of molecular structures from ground state rotational constants, *J. Chem. Phys.* 29 (1958) 864–874, <https://doi.org/10.1063/1.1744602>.